OPEN

RETINAL TECTONICS AFTER MACULAR PUCKER SURGERY

Thickness Changes and *En Face* Displacement Recovery

FABIO SCARINCI, MD,* GIORGIO QUERZOLI, PHD,† PAMELA COSIMI, MD,*
GUIDO RIPANDELLI, MD,* MARIO R. ROMANO, MD, PHD,‡ ANDREA CACCIAMANI, MD,*
MARION R. MUNK, MD,§¶** TOMMASO ROSSI, MD*

Purpose: To study visual function, retinal layer thickness changes, and tangential displacement after pars plana vitrectomy for epiretinal membrane.

Methods: Retrospective series of patients undergoing pars plana vitrectomy for epiretinal membrane, with 6-month follow-up including best-corrected visual acuity, optical coherence tomography, M-charts, epiretinal membrane grading, and infrared fundus photograph at time 0 (T0, preop) at months 1 (T1), 3 (T3), and 6 (T6) postop (±1 week). Retinal layer thickness and tangential (*en face*) retinal displacement between successive times for the entire retinal surface and the central horizontal and vertical meridian were also measured. *En face* displacement was calculated as optical flow of consecutive images.

Results: Average best-corrected visual acuity improved from 0.28 ± 0.08 logarithm of Minimum Angle of Resolution at T0 to 0.16 ± 0.25 at T6 ($P = 0.05$), best-corrected visual acuity improvement correlated with best corrected visual acuity (BCVA) at T0 ($P < 0.001$). Vertical metamorphopsia decreased from 1.33° ± 0.70° at T0 to 0.82° ± 0.69° at T6 ($P < 0.05$). Foveal thickness reduced from 453 ± 53 μm at T0 to 359 ± 31 μm at T6 ($P < 0.05$) and reduction correlated with best-corrected visual acuity improvement ($P < 0.05$). Foveal layers decreased ($P < 0.05$) in all cases. The mean *en face* deformation was 155.82 ± 50.17 μm and mostly occurred in the first month: T0-T1 displacement was 83.59 ± 30.28 μm, T1–T3 was 36.28 ± 14.45 μm, while T3–T6 was 39.11 ± 22.79 μm ($P < 0.001$) on average. Perifoveal and parafoveal deformation correlated with optical coherence tomography foveal thickness reduction at all time intervals (1, 3, and 6 months: $P < 0.01$).

Conclusion: Epiretinal membrane peeling affects all retinal layer thickness and results in new force balance across the entire retina and tangential displacement. Both *en face* and in-depth changes correlate with visual function.

RETINA 44:102–110, 2024

Idiopathic macular pucker is a pathologic condition due to the anomalous or incomplete posterior vitreous detachment leaving posterior hyaloid remnants adherent to the retinal surface,[1] more accurately referred to as idiopathic epiretinal membranes (ERMs). The subsequent contraction of adherent vitreous may exert tangential traction over the inner and outer retina, causing irregular retinal displacement, macular thickening, and visual disturbance.[2]

Metamorphopsia defined as the deformation of visual perception[3] and the deterioration of visual acuity are the functional hallmarks of symptomatic ERMs and may affect patients' quality of life[4] prompting surgical removal.

Metamorphopsia has been ascribed to the degree of retinal layer disorganization and the misalignment of retinal layers causing Müller cells bending in EMRs,[5,6] diabetic macular edema,[7] and retinal vein occlusion[8]; however, the precise attribution of visual symptoms to anatomical changes remains elusive.

Pars plana vitrectomy with ERM peeling may reduce the retinal deformation, decrease metamorphopsia, and improve visual acuity.[9] The mechanism underlying the reduction of metamorphopsia and the recovery of vision has not yet been fully elucidated; however, it has been associated with cellular function recovery and microarchitectural changes.[10]

The purpose of this study was to evaluate retinal layers' thickness changes and in-plane ("*en face*") displacement after pars plana vitrectomy and their association with visual function: visual acuity and metamorphopsia.

Materials and Methods

Study Participants

We retrospectively analyzed all patients undergoing pars plana vitrectomy and peeling for idiopathic ERM affecting the fovea classified as stage 2 to stage 3 according to Govetto[11] with a disease duration <3 years. All patients received surgery at the IRCCS Bietti Foundation between January and June 2022 and had been operated by a single surgeon. Diagnosis was confirmed by ophthalmoscopic examination and spectral domain optical coherence tomography (SD-OCT). This study was conducted at the Ophthalmology Department of the Bietti Foundation between January and November 2022.

Exclusion criteria were as follows: (1) history of ocular and specifically macular disorders including age-related macular degeneration, retinal vascular occlusions, retinal detachment, trauma, high myopia (ocular axial length >26.00 mm), and uveitis; (2) history of systemic diseases, including hypertension and diabetes; (3) poor imaging quality due to media opacity; and (4) incomplete chart or records.

Seventeen patients (10 females and 7 males) met inclusion criteria and received complete ophthalmologic assessment, patent and manifest refraction, best-corrected visual acuity (BCVA) using Early Treatment Diabetic Retinopathy Study acuity charts, and Snellen visual acuity converted to the logarithm of Minimum Angle of Resolution units for statistical purposes and indirect ophthalmoscopy. The degree of horizontal and vertical metamorphopsia was assessed using M-CHARTS (Inami, Co, Tokyo, Japan)[12]; retinal sensitivity was obtained with microperimetry, and SD-OCT scan was also performed. All included patients had the above information available at time 0 (pre-op), times 1, 3, and 6 months (±7 days) after surgery.

All patients provided written informed consent, and the study adhered to the tenets of the Declaration of Helsinki and received approval of the local Ethics Committee (ERMLAB01 N° 77/18/FB).

Surgical Procedure

All patients underwent a standard 25-gauge 3-port pars plana vitrectomy with ERM and internal limiting membrane (ILM) peeling with single Brilliant Blue G staining (Kemin Pharmaceutica Unipessoal, LTDA, Des Moines, IA).

Optical Coherence Tomography Image Acquisition

Spectral domain optical coherence tomography (SPECTRALIS HRA-OCT, version 1.5.12.0; Heidelberg Engineering, Heidelberg, Germany) images were acquired using the horizontal SD-OCT cross-section (an average of 25–30 frames for each B-scan was used to improve image quality as elsewhere reported[13]). Baseline acquisitions were taken before surgery (T0) and repeated with follow-up function set at 1 month (T1), 3 months (T3), and 6 months (T6) post-surgery. Before data assessment, the extract centration and location of the OCT scan was checked and if needed manually corrected. The segmentation of the retina was obtained using automatic built-in software, and all SD-OCT scans were segmented into four layers as described in ref. 14. Owing to the pathologic changes induced by the ERM itself, the inner retinal layers appeared at times indistinguishable in OCT images. For this reason, we cumulatively defined as "Inner Retina", the most inner layer comprising the ILM + retinal nerve fiber layer, the ganglion cell layer, and inner plexiform layer (IRL = ILM + retinal nerve fiber layer + ganglion cell layer + inner plexiform layer). The central 1-mm foveal thickness, inner nuclear layer (INL), outer plexiform layer, and outer nuclear layer remained always distinguishable in OCT and were therefore analyzed as such.

Retinal layer thickness considered in the analysis were also divided by EDTRS sectors: foveal central 1 mm, superior, temporal, inferior, and nasal. Concentric circles indicated the foveolar region (radius 0.5 mm), perifoveal (radius 1.5 mm), and parafoveal (radius 3 mm).

Measurements of the Retinal En Face Deformation

En face dislocation was measured by comparing couples of successive images taken at baseline (month

From the *IRCCS Fondazione Bietti ONLUS, Roma, Italy; †DICAAR—Università di Cagliari, Italy; ‡Department of Biomedical Science, Humanitas University, Milan, Italy; §Augenarzt-Praxisgemeinschaft Gutblick AG, Pfäffikon. Switzerland; ¶Feinberg School of Medicine, Northwestern University, Chicago, Illinois; and **Department of Ophthalmology, Inselspital, University Hospital Bern, Bern, Switzerland.

None of the authors has any financial/conflicting interests to disclose.

Reprint requests: Tommaso Rossi, MD, IRCCS Fondazione Bietti ONLUS, Via Livenza 3, 00198 Roma, Italy; e-mail: tommaso.rossi@usa.net

0) and after 1, 3, and 6 months. Thus, we present and discuss the deformation during the first month after surgery (T0–T1), the successive 2 months (T1–T3), and the additional 3 months (T3–T6). Displacements between consecutive images were computed on a regular grid (36 × 36 nodes) using the Farneback two-frame motion estimation method,[15] which is based on the idea of comparing the neighborhoods of corresponding nodes on the two images to find the translation between them. Preliminarily, the grey levels of the images were inverted and preprocessed to obtain a uniform enhancement of the details over the single image and between images. Small image portions were independently analyzed, and the contrast was locally modified to obtain a uniformly flat intensity histogram. Then, each couple of images was corrected for a rigid roto-translation to discard the differences due to the different orientation and centration of the two analyses and thus obtain two perfectly aligned images. At that aim, (i) the map of the two-component displacements was computed by the Farneback algorithm, (ii) the roto-translation minimizing the sum of the square differences of the 36 × 36 calculated displacements was found, (iii) the roto-translation was applied to the second image to subtract the misalignment between them, and (iv) the above procedure (consisting of steps ii and iii) was iterated until convergence (i.e., when sum of the square differences varied less than 3% between two consecutive iterations). After the roto-translation removal, the retinal deformation was obtained on the same grid by using again the displacement detection algorithm. The small marginal nonoverlapping regions at the borders of the images were excluded from the latter step.

We analyzed the results (shown as vector fields) both over the whole image and in the regions of interest shown in Figure 1: the circular region 0.5 mm in radius, (hereafter referred to as "central"), two circular crowns with the same center and radius ranging from 0.5 mm to 1.5 mm ("perifoveal") and from 1.5 up to 3 mm ("parafoveal"), and the 1-mm wide region adjacent to a horizontal and a vertical line crossing on the foveola (horizontal and vertical meridian, respectively). To let the reader visually perceive the changes, in Figure 1, as well in the following figures, we superimposed the two analyzed images using pseudo-colors: The first image is red while the second is green. Thus, red represents details that were present only in the first image while green represents details present only in the second image. Details present in both images (indicating that no changes occurred during the considered time) results in yellow (i.e., red+green).

The two components (*Dx*, horizontal and *Dy*, vertical) of the displacement are obtained in microns, and

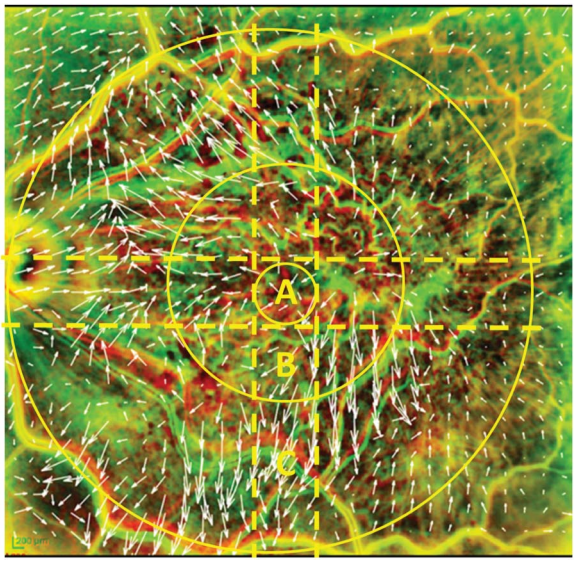

Fig. 1. Regions used to analyze the retinal deformation. The yellow lines indicate (**A**) the "central" circular region, 0.5 mm in diameter; (**B**) the "perifoveal" annular ring with 0.5 mm and 1.5 mm inner and outer diameters, respectively; (**C**) the "parafoveal" annular ring with 1.5 mm and 3 mm inner and outer diameters, respectively. The dashed lines indicate the horizontal and vertical 1-mm wide regions intersecting on the foveola. The background represents in pseudo-colors two consecutive images of patient #3 (T0 and T1). The first image is in red while the second image is in green. As a result, red indicates details present only in the first image, green indicates details present only in the second image while details persisting in both images results yellow. White arrows represent the vector displacement in magnitude and direction.

the statistics such as mean values are computed using the displacement magnitude of the vectors $D = \sqrt{Dx^2 + Dy^2}$ included in the region of interest (the whole image or one of the above mentioned).

Main Outcome Measures

Main study outcome measures included BCVA, M-charts grading, microperimetric retinal sensitivity, retinal layers thickness, overall foveal thickness, mean *en face* displacement, and the correlation between functional and anatomical changes.

Statistical Analysis

The analysis of variance with *t*-test and *t*-test for repeated measures applied to numerical variables was used to assess changes at different time points. Bivariate Pearson's r correlation coefficient was applied for continuous variables while Spearman's rho and Kendall's Tau were used for the assessment of ordinal variables such as ERM classification grades. The Shapiro–Wilk test was used for the Gaussian distribution of data.

In all cases, P values < 0.05 were considered statistically significant.

Results

Visual Acuity and Metamorphopsia

Sample population included 17 patients (7 males and 10 females); the mean age was 74.8 ± 7.9 years with no significant difference between sexes. Average BCVA significantly improved from 0.28 ± 0.08 logarithm of Minimum Angle of Resolution at T0 to 0.16 ± 0.25 at T6 months (0.49–0.68 Snellen; $P < 0.05$) and BCVA improvement correlated with BVCA at T0 ($P < 0.001$; Table 1).

Horizontal metamorphopsia did not change significantly (0.91° ± 0.70° at T0 vs. 0.78° ± 0.56° at 6 months; n.s.) while vertical metamorphopsia decreased during the study follow-up (1.33° ± 0.70° at T0 vs. 0.82° ± 0.69° at T6; $P < 0.05$).

Retinal Layer Thickness Changes

The overall foveal thickness reduced from 453 ± 53 at T0 to 359 ± 31 μm at T6 months and the amount of thickness reduction correlated with BCVA improvement ($P < 0.05$). Most of the foveal thinning was due to the inner retinal layer thickness reduction, which significantly decreased in each considered Early Treatment Diabetic Retinopathy Study sector ($P < 0.05$ in all cases; Figure 2). Thickness reduction correlated with ERM grading ($P < 0.016$).

All other deeper retinal layers showed only sectorial significant thinning shown in Figure 3: The INL and outer plexiform layer of the central foveolar, superior, and temporal subfield sectors reduced their thickness at the INL and outer plexiform layer thickness decreased ($P < 0.05$) while only the outer nuclear layer thickness of the central foveolar subfield significantly decreased during this study ($P < 0.05$; Figure 3).

Retinal En Face Displacement

En face displacement magnitude averaged over the entire central field and the 6-month follow-up was 155.82 ± 50.17 μm. Displacement mostly occurred during the first month postsurgery: mean displacement was 83.59 ± 30.28 μm between T0–T1 versus 36.28 ± 14.45 μm between T1–T3 ($P < 0.001$) and 39.11 ± 22.79 μm between T3–T6 (not significant; Table 2). All considered concentric regions underwent a significantly higher displacement within the first month ($P < 0.05$ for all) and displacement increased with eccentricity because the annular ring with radius ranging from 1.5 mm to 3 mm suffered a higher average displacement compared with the fovea in the first 3 months (Table 2; $P < 0.01$ in all cases).

The en face deformation along the "central cross" was 36 ± 13 μm across the horizontal and 41 ± 14 μm across the vertical meridian, the difference being not statistically significant.

Perifoveal and parafoveal deformation correlated with SD-OCT foveal thickness reduction at all time intervals (T0–T1, T1–T3, and T3–T6; $P < 0.01$ for all). Both overall foveal and IRL thinning strongly correlated with the *en face* displacement ($P < 0.01$ for both).

En face displacement did not correlate with BCVA or microperimetric retinal sensitivity. The displacement along the vertical line correlated with the improvement in horizontal metamorphopsia ($P < 0.028$). The distribution of *en face* displacement compared with visual acuity changes, followed a Gaussian normal distribution ($P < 0.05$; Figure 4). *En face* displacement also correlated with deeper layers thickness decrease such as INL central ($P = 0.007$), INL perifoveal nasal ($P = 0.011$), and outer nuclear layer central ($P = 0.012$).

Epiretinal membranes classification correlated with the overall tangential deformation ($P = 0.019$) and vertical and horizontal retinal deformation ($P < 0.01$ for both).

BCVA at T0 correlated with the perifoveal ($P = 0.036$) and parafoveal ($P = 0.04$) *en face* deformation in T3-T6. M-charts scoring change between any given time point does not correlate either with BCVA improvement, retinal thickness changes, or *en face* retinal deformation over the whole investigation region.

Table 1. BCVA, Metamorphopsia, and Microperimetric Sensitivity Throughout Follow-Up

	T0	T1	T3	T6	*P*
Visual acuity (Snellen)	0.49 ± 0.13	0.55 ± 0.25	0.62 ± 0.23	0.68 ± 0.12	<0.05
Horizontal metamorphopsia (°)	0.91 ± 0.70	0.87 ± 0.48	0.72 ± 0.17	0.78 ± 0.56	n.s.
Vertical metamorphopsia (°)	1.33 ± 0.70	1.34 ± 0.57	0.84 ± 0.74	0.82 ± 0.69	<0.05
Microperimetric sensitivity mean (db)	23.1 ± 4.4	21.2 ± 7.1	22.0 ± 6.5	21.4 ± 7.6	n.s.
Microperimetric sensitivity 5° (db)	20.7 ± 4.1	20.24 ± 5.6	21.1 ± 4.7	20.9 ± 5.8	n.s.
Microperimetric sensitivity 10° (db)	22.9 ± 4.4	19.7 ± 8.3	22.1 ± 5.7	21.8 ± 6.7	n.s.

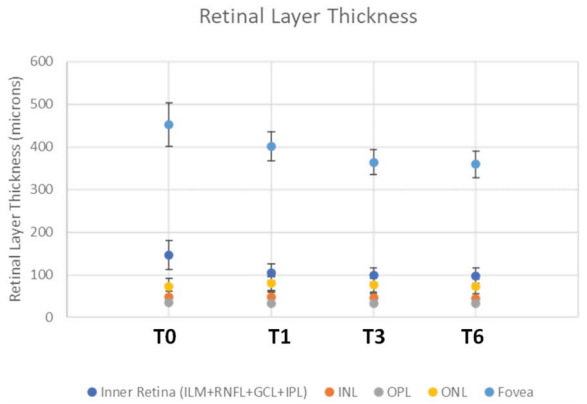

Fig. 2. Retinal layer and entire foveal thickness changes across follow-up. Note how most of the thickness changes occur in the IR. IR, inner retina.

Discussion

Pars plana vitrectomy with ERM peeling can stop disease progression and improve vision and metamorphopsia[16]; however, the underlying ultrastructural mechanisms remain poorly understood.[17]

Our data confirm that ERM is a full-thickness disease and peeling affects the whole retina, affecting both inner and outer layers (Figure 3); similarly, the degree of retinal disruption graded by the ERM classification[12] correlated with *en face* displacement and postoperative thickness reduction at all levels.

Peeling maneuvers released the internal tensions of the tissue, thus modifying the postoperative retinal structure three-dimensionally, a process more pronounced in the first 30 days but spanning over the entire 6 months of follow-up time (Figure 5). It should be emphasized that the new equilibrium causes the postoperative displacement along the three axis and does not necessarily (and teleologically) imply either anatomical or functional restoration, as shown in Figure 6, where despite 100 μm of postoperative foveal thinning (Figure 6D), metamorphopsias increased between T3 and T6 while BCVA remained unchanged (Figure 6E).

Interestingly, an average 93 μm loss of foveal thickness, resulted in 148 μm of average *en face* displacement (Table 2), unevenly distributed over the retinal surface and more pronounced at the parafoveal level (165 μm), compared with the fovea (104 μm). Chen and Coll,[18] demonstrated that vessels contribute significantly to retinal stiffness and "[. . .] *vessel size is the only determining factor that governs the anisotropic and inhomogeneous characteristics of the retina*."

Although the functional benefit of ILM peeling performed in our series, compared with ERM stripping

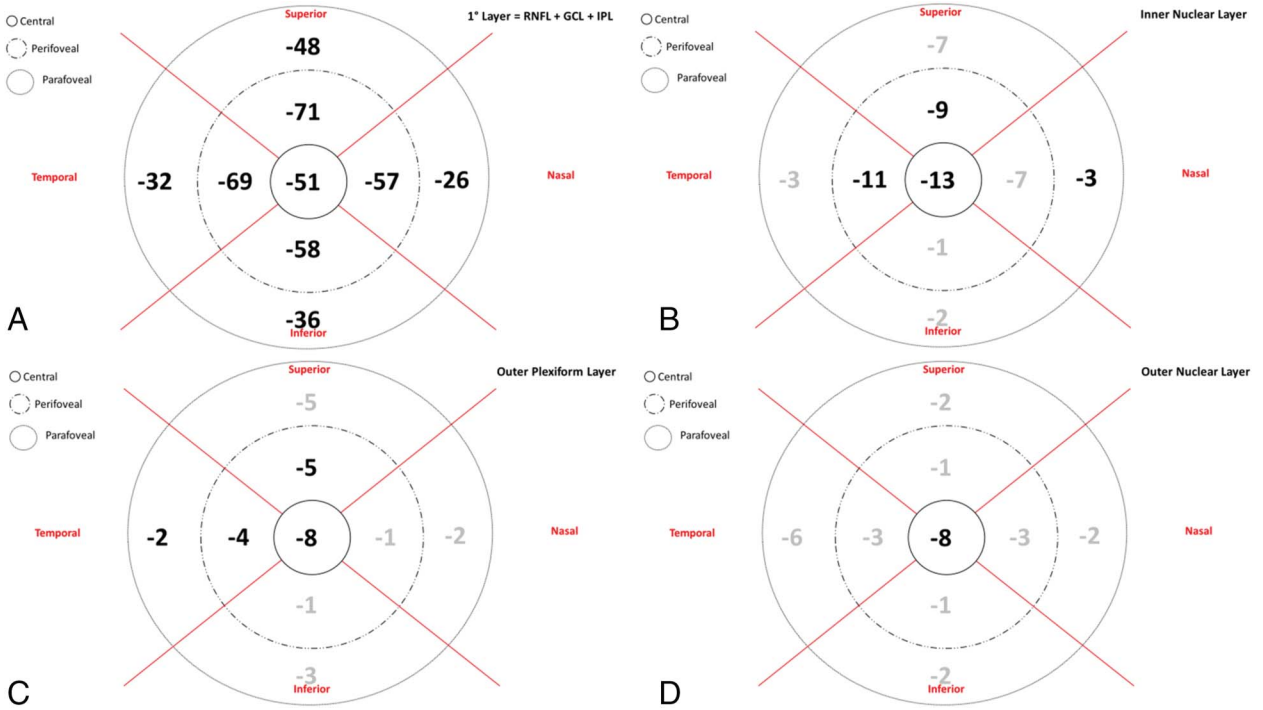

Fig. 3. Retinal layer thickness changes (T0–T6) from inner to outer retina and divided by sectors: central foveolar, superior, temporal, inferior, and nasal. **A.** IR (ILM + RNFL + GCL + IPL) including RNFL, GCL, and IPL; (**B**) INL; (**C**) OPL; and (**D**) ONL. Concentric circles indicate the foveolar region (radius 0.5 mm), perifoveal (radius 1.5 mm), and parafoveal (radius 3 mm). Numbers indicate thickness changes (in microns), and bold numbers indicate a significant reduction in thickness ($P < 0.05$ for all). GCL, ganglion cell layer; IPL, inner plexiform layer; IR, inner retina; ONL, outer nuclear layer; OPL, outer plexiform layer; RNFL, retinal nerve fiber layer.

Table 2. *En face* Displacement in Microns, Throughout Follow-Up of Central 6 × 6 mm Field and Concentric EDTRS Areas

	0–1 month	1–3 months	3–6 months	0–6 months
Central foveal thickness change	−52.4 ± 136.8	−38.3 ± 46	−2.58 ± 43.3	−93.3 ± 124.1
Overall displacement (6 × 6 mm field)	83.5 ± 30.2	36.2 ± 14.4	39.1 ± 22.7	148.8 ± 24.1
Central circle (0.5 mm radius)	46.4 ± 28.4	22.9 ± 18.3	30.5 ± 19.0	104.7 ± 25.3
Perifoveal crown (1.5 mm radius)	62.3 ± 37.5	67.8 ± 38.2	29.5 ± 16.4	159.6 ± 29.1
Parafoveal crown (3 mm radius)	82.4 ± 52.7	50.0 ± 28.1	33.2 ± 18.1	165.6 ± 31.4

alone, remains uncertain,[19] from the mechanical standpoint, ILM removal is very likely to trigger significant retinal adjustments because the ILM is a stiff structure[20] whose properties change after peeling and also with staining.[21] A recent meta-analysis reported a significantly thicker postoperative fovea in patients undergoing ILM peeling compared with ERM peeling alone.[22]

The retinal vessels, therefore, represent a true "backbone" responsible for *en face* displacement that could be exacerbated by ILM removal and whose impact on retinal microcircuitry is unknown. Glial and Müller cells activation progressing from inner to outer retina in response to ERMs has been previously described[23] and further modifies the mechanical properties and the response to surgery.

From a purely geometric perspective, 150 μm of *en face* displacement exceed the linear dimension of Müller cells and are very likely to determine synaptic disconnection, leading to visual loss. The reason why such macroscopic displacement does not affect vision more profoundly is debatable and may relate to the chronicity of its development and possibly to rewiring processes,[24] still to be documented. Another reason may lay in the uncertain attribution of *en face* displacement within the retinal thickness.

The *en face* displacement we report, in fact, refers to infrared images where all retinal layers are considered at the same time. Thus, calculated vectors may belong to different layers such as the superficial and deep capillary *plexi*. This notion does not affect the accuracy of displacement itself but cannot localize accurately its depth, which implies a much higher and three-dimensional level of complexity, still to be understood.

However, displacement vectors in Figures 5 and 6 show elements overtly laying at different depths moving at different rates and directions, unpredictably kinking cells spanning the z-axis: photoreceptors, bipolar, ganglion, and Müller cells.

This dynamic scenario may be responsible for the controversial relation between visual function and anatomy[9]: *En face* displacement along the vertical line of the cross correlated with the change in horizontal metamorphopsia; however, the displacement along the horizontal line did not correlate with vertical M-charts scoring. *En face* displacement correlated with retinal thinning but not to BCVA improvement, as already reported by Matsumoto[25] in his original article. This finding may suggest that, apart from thinning, cellular bending also occurring at the level of the z-axis (perpendicular to our *en face* displacement measures) may play a decisive functional role.

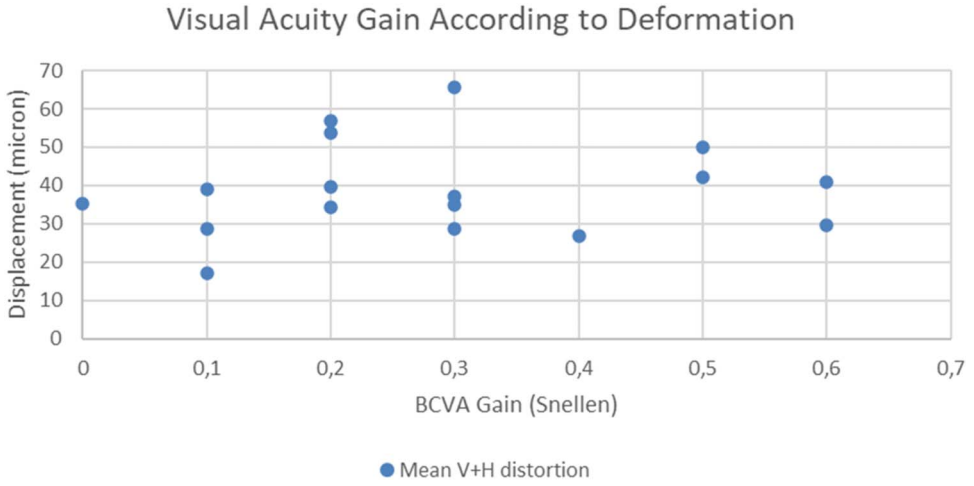

Fig. 4. Distribution of mean *en face* displacement data as a function of BCVA increase.

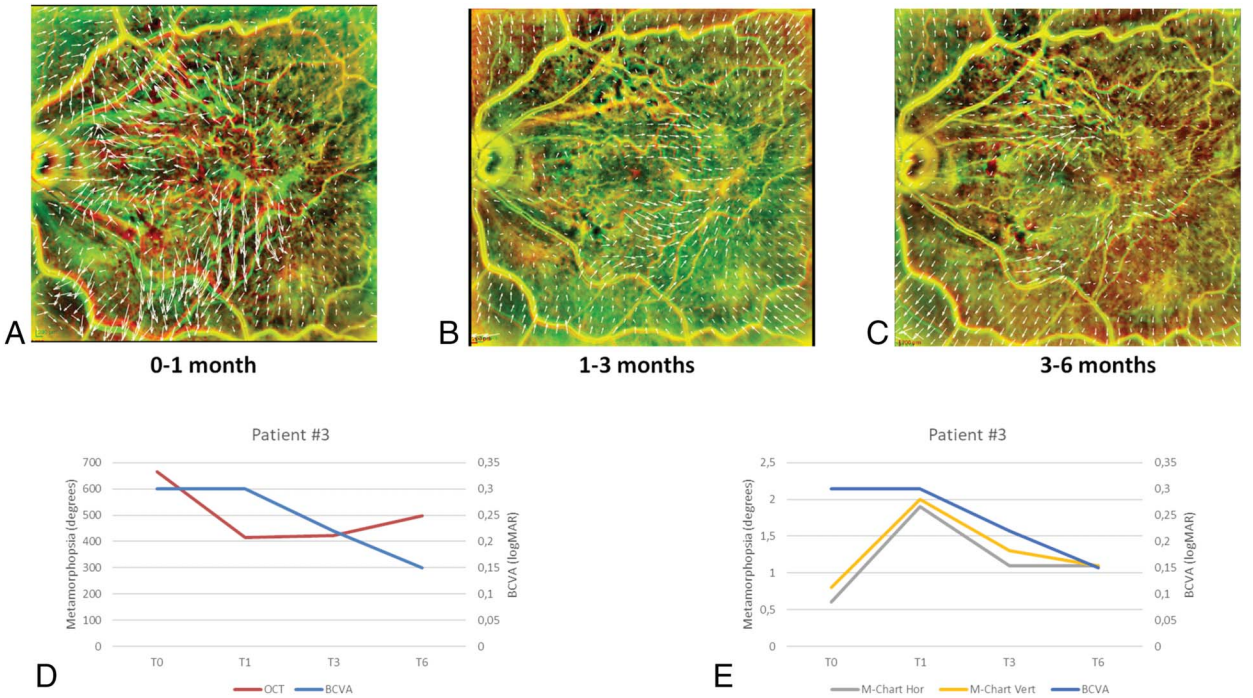

Fig. 5. Patient #3. Color pictures show *en face* displacements during (**A**) T0–T1; (**B**) T1–T3; (**C**) T3–T6. Inferior graphs show (**D**) BCVA and OCT foveolar thickness during follow-up; (**E**) vertical and horizontal metamorphopsia compared with BCVA during follow-up. Most *en face* displacement occurred during T0–T1 (**A**) but the fovea kept moving up to T6. Interestingly, despite OCT foveal thinning, BCVA did not improve during T0–T1 (panel d) as metamorphopsias worsened during that time (e).

Mieno and Coll[26] found similar results and even Amsler in 1953 reported[27] a greater deformation for horizontal lines than vertical; it is worth mentioning that vertical deformation affects horizontal line perception and vice versa. Allegrini and Coll[28] measured the displacement of retinal vascular junctions after ERM peeling and found a significant correlation with BCVA changes. As for this study, most changes in both BCVA and *en face* displacement occurred during the first month postsurgery (Figures 5 and 6), indicating that retinal motion is the primary factor affecting BCVA.

Previous studies suggest that traction induces intraretinal changes mediated by macroglia activation[11] which in turn overexpress glial fibrillary acid proteins in the IRL, resulting in intraretinal gliosis and the binding between Müller cells and the ILM.[29] Our study also supports these findings because IRL thinning and *en face* displacements highly correlated ($P < 0.001$) after ERM peeling.

It is conceivable that if gliosis progresses too deep into the retina, it will no longer be able to recover, despite ERM peeling, to the detriment of the nervous elements. Therefore, the ideal surgical timing could be when the retina is still able to move and the intraretinal gliosis has not propagated too deep into the retinal layers.

Displacement behavior as a function of BCVA gain (Figure 4) may support this hypothesis, although the Gaussian distribution of *en face* displacement may well be a mere feature of pathology itself (as for many distributions). Patients showing the highest and lowest grades of *en face* displacement equally gained less vision, the former subgroup likely due to their greater initial compromission and the latter for a "ceiling" effect related to their relatively good preop vision. Patients obtaining the highest vision improvement, vice versa, belong to the intermediate displacement subgroup, possibly because they started with low vision but less compromised anatomical conditions and/or reversible gliosis. If this held true, the postoperative retinal displacement would be a proof a reversible grade of gliosis and better visual prognosis.

In summary, our study introduced for the first time an accurate and objective measure of *en face* displacement, demonstrating how deeply the removal of ERMs affects the entire 3D retinal architecture. Although the major pitfall is the inability to discern the diverse layers on retinal photographs, we believe the incomparably greater number of points examined, offer much greater information, and set the base for further studies.

Finally, we should acknowledge that the concept of surgery as a mechanism of *restitutio* ad int*egrum* is

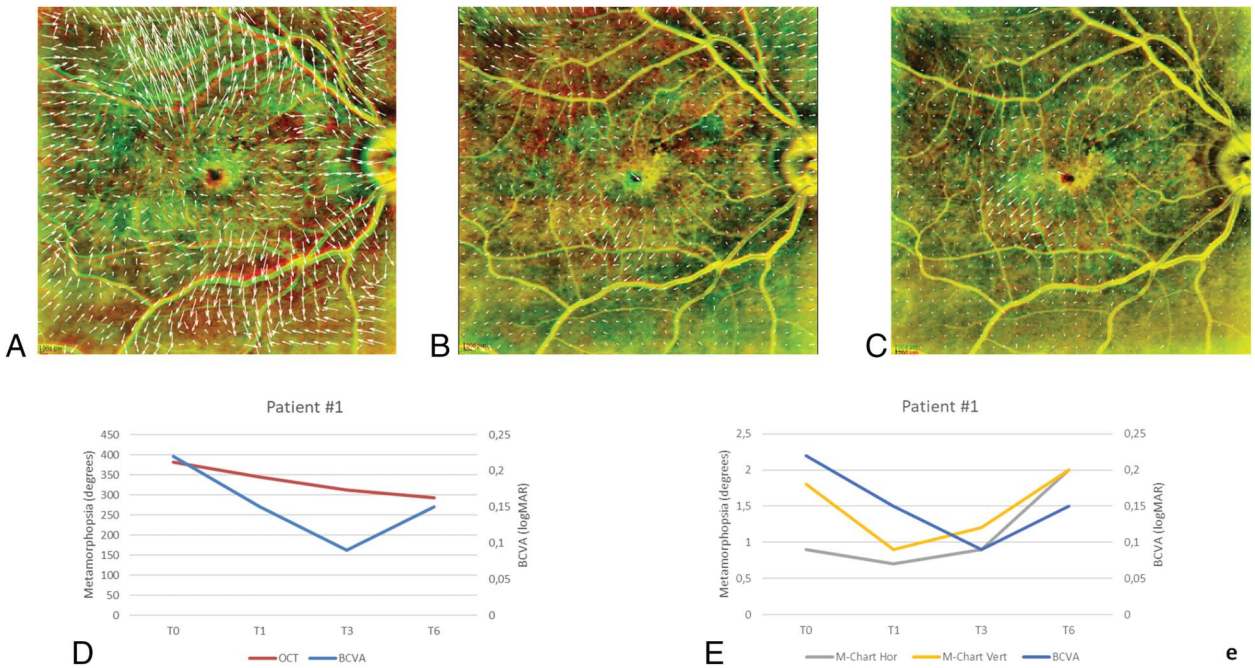

Fig. 6. Patient #1. Color pictures show *en face* displacements during (**A**) T0–T1; (**B**) T1–T3; (**C**) T3–T6. Lower graphs show (**D**) BCVA and OCT foveolar thickness during follow-up; (**E**) vertical and horizontal metamorphopsia compared with BCVA during follow-up. Note that despite the reduction of foveal thickness, BCVA increased up to T3 and worsened at T6 while metamorphopsias increased since T1 after the initial improvement.

misleading: With all the uncertainties of biomechanical measures, the properties of the entire retina,[30] isolated ILM,[20] and ERM[31] are significantly different and span two orders of magnitude; stripping the ERM and ILM from the retinal surface means removing thick and stiff structures adherent to the retina, thus macroscopically altering the balance of forces. By no means, this can be simplified as "rewinding" the course of disease.

As a final remark, we notice that it will be necessary to expand a detailed assessment of the *en face* displacement for each retinal layer both before and after surgery to comprehend the functional damage at a cellular level and predict visual outcome and possibly infer the ideal surgical timing.

Key words: metamorphopsia, epiretinal membrane, macular pucker, retinal layer.

Acknowledgments

The authors thank the "Fondazione Roma" and the Italian Ministry of Health for financial support. The authors would thank Giuliana Facciolo and Francesca Petruzzella for patient study and image analysis.

References

1. Fung AT, Galvin J, Tran T. Epiretinal membrane: a review. Clin Exp Ophthalmol 2021;49:289–308.
2. Bringmann A, Unterlauft JD, Barth T, et al. Foveal configurations with disappearance of the foveal pit in eyes with macular pucker: presumed role of Müller cells in the formation of foveal herniation. Exp Eye Res 2021;207:108604.
3. Simunovic MP. Metamorphopsia and its quantification. Retina 2015;35:1285–1291.
4. Xu K, Gupta V, Bae S, Sharma S. Metamorphopsia and vision-related quality of life among patients with age-related macular degeneration. Can J Ophthalmol 2018;53:168–172.
5. Ichikawa Y, Imamura Y, Ishida M. Inner nuclear layer thickness, a biomarker of metamorphopsia in epiretinal membrane, correlates with tangential retinal displacement. Am J Ophthalmol 2018;193:20–27.
6. Sakai D, Takagi S, Hirami Y, et al. Correlation between tangential distortion of the outer retinal layer and metamorphopsia in patients with epiretinal membrane. Graefes Arch Clin Exp Ophthalmol 2021;259:1751–1758.
7. Nakano E, Ota T, Jingami Y, et al. Correlation between metamorphopsia and disorganization of the retinal inner layers in eyes with diabetic macular edema. Graefes Arch Clin Exp Ophthalmol 2019;257:1873–1878.
8. Chan EW, Eldeeb M, Sun V, et al. Disorganization of retinal inner layers and ellipsoid zone disruption predict visual outcomes in central retinal vein occlusion. Ophthalmol Retina 2019;3:83–92.
9. Chang S, Gregory-Roberts EM, Park S, et al. Double peeling during vitrectomy for macular pucker: the Charles L. Schepens Lecture. JAMA Ophthalmol 2013;131:525–530.
10. Zeyer JC, Parker P, Dajani O, MacCumber MW. Preoperative domed macular contour correlates with postoperative visual gain after vitrectomy for symptomatic epiretinal membrane. Retina 2021;41:505–509.
11. Govetto A, Lalane RA III, Sarraf D, et al. Insights into epiretinal membranes: presence of ectopic inner foveal layers and a new optical coherence tomography staging scheme. Am J Ophthalmol 2017;175:99–113.

12. Arimura E, Matsumoto C, Nomoto H, et al. Correlations between M-CHARTS and PHP findings and subjective perception of metamorphopsia in patients with macular diseases. Invest Ophthalmol Vis Sci 2011;52:128–135.
13. Parravano M, De Geronimo D, Scarinci F, et al. Progression of diabetic microaneurysms according to the internal reflectivity on structural optical coherence tomography and visibility on optical coherence tomography angiography. Am J Ophthalmol 2019;198:8–16.
14. Cacciamani A, Cosimi P, Di Nicola M, et al. Correlation between outer retinal thickening and retinal function impairment in patients with idiopathic epiretinal membranes. Retina 2019;39:331–338.
15. Farneback G. "Two-frame motion estimation based on polynomial expansion". In Proceedings of the 13th Scandinavian Conference on Image Analysis, 2003, Halmstad, Sweden: SCIA, 363–370.
16. Nguyen JH, Yee KM, Sadun AA, Sebag J. Quantifying visual dysfunction and the response to surgery in macular pucker. Ophthalmology 2016;123:1500–1510.
17. Chua PY, Sandinha MT, Steel DH. Idiopathic epiretinal membrane: progression and timing of surgery. Eye (Lond). 2022; 36:495–503.
18. Chen K, Weiland JD. Anisotropic and inhomogeneous mechanical characteristics of the retina. J Biomech 2010;43:1417–1421.
19. Fang XL, Tong Y, Zhou YL, et al. Internal limiting membrane peeling or not: a systematic review and meta-analysis of idiopathic macular pucker surgery. Br J Ophthalmol 2017;101:1535–1541.
20. Vielmuth F, Schumann RG, Vetal S, et al. Biomechanical properties of the internal limiting membrane after intravitreal ocriplasmin treatment. Ophthalmologica 2016;235:233–240.
21. Haritoglou C, Mauell S, Benoit M et al. Vital dyes increase the rigidity of the internal limiting membrane. Eye (Lond). 2013; 27:1308–1315.
22. Sun Y, Zhou R, Zhang B. With or without internal limiting membrane peeling for idiopathic epiretinal membrane: a meta-analysis of randomized controlled trials. Retina 2021;41:1644–1651.
23. Bringmann A, Unterlauft JD, Barth T, et al. Müller cells and astrocytes in tractional macular disorders. Prog Retin Eye Res 2022;86:100977.
24. Gao H, Huang X, He J, et al. The roles of microglia in neural remodeling during retinal degeneration. Histol Histopathol 2022;37:1–10.
25. Matsumoto C, Arimura E, Okuyama S, et al. Quantification of metamorphopsia in patients with epiretinal membranes. Invest Ophthalmol Vis Sci 2003;44:4012–4016.
26. Mieno H, Kojima K, Yoneda K, et al. Evaluation of pre- and post-surgery reading ability in patients with epiretinal membrane: a prospective observational study. BMC Ophthalmol 2020;20:95.
27. Amsler M. Earliest symptoms of diseases of the macula. Br J Ophthalmol 1953;37:521–537.
28. Allegrini D, Montesano G, Marconi S, et al. A novel quantitative analysis method for idiopathic epiretinal membrane. PLoS One 2021;16:e0247192.
29. Romano MR, Ilardi G, Ferrara M, et al. Intraretinal changes in idiopathic versus diabetic epiretinal membranes after macular peeling. PLoS One 2018;13:e0197065.
30. Ferrara M, Lugano G, Sandinha MT et al. Biomechanical properties of retina and choroid: a comprehensive review of techniques and translational relevance. Eye (Lond) 2021;35:1818–1832.
31. Ciasca G, Pagliei V, Minelli E, et al. Nanomechanical mapping helps explain differences in outcomes of eye microsurgery: a comparative study of macular pathologies. PLoS One 2019. 14;e0220571.